Biological Polynuclear Clusters Coupled by Magnetic Interactions: From the Point Dipole Approximation to a Local Spin Model

Patrick Bertrand,*,† Claude More,† Bruno Guigliarelli,† André Fournel,† Brian Bennett,‡ and Barry Howes‡

Contribution from the Laboratoire d'Electronique des Milieux Condensés, CNRS ER 28, Université de Provence, Centre Saint Jérôme, case 241, 13397 Marseille cedex 13, France, and School of Chemistry and Molecular Sciences, The University of Sussex, Brighton BN1 9QJ, U.K.

*Received September 13, 1993**

Abstract: The structural organization of paramagnetic centers in biomolecules can be predicted on the basis of a quantitative study of their magnetic interactions. These studies are usually carried out within the framework of the so-called point dipole approximation, in which the delocalization of the magnetic moments over the centers is ignored. In this paper, we examine how this delocalization can be taken into account in the spin Hamiltonian describing the magnetic interactions between polynuclear paramagnetic centers. A *local spin* model is described and applied first to a system made of a dinuclear center interacting with a mononuclear center and then to a system comprising two dinuclear centers. In both cases, the EPR spectrum calculated from the *local spin* model is compared to that given by the point dipole model for different geometrical configurations. The model is illustrated by a detailed quantitative study of the magnetic interactions between the molybdenum center and one [2Fe–2S] center (center 1) in the enzyme xanthine oxidase. These studies emphasize the *effective* character of some important structural parameters given by numerical simulations of EPR spectra based on the point dipole approximation.

Introduction

There is a large class of prosthetic groups in proteins which possess an oxidation state in which they are paramagnetic. This includes organic entities like flavins or quinones and inorganic complexes built from various transition-metal ions. As a consequence, magnetic techniques like EPR, ENDOR, and Mössbauer spectroscopies have played an essential role in their characterization. It is often possible to prepare the systems containing such groups in a redox state in which neighboring centers are simultaneously paramagnetic. In these conditions, the intercenter magnetic interactions give rise to a complex EPR spectrum, the shape of which is strongly dependent on the distance and the relative orientation of the centers. The detailed study of these magnetic interactions, based on the simulation of spectra recorded at different microwave frequencies, constitutes a very promising method for obtaining structural information on these systems. As a matter of fact, a number of such studies have already appeared in the literature.[1-9]

In the model that is generally used to describe the magnetic interactions between two centers A and B, the magnetic moments μ_A and μ_B are approximated by point dipoles whose relative position is defined by a unit vector $\vec{u}_{AB}$ and a distance r_{AB}. The spin Hamiltonian is then written:[10]

$$\mathcal{H}_{int} = \mathcal{H}_z + \mathcal{H}_{ex} + \mathcal{H}_{dip}$$

$$\mathcal{H}_z = -\vec{\mu}_A\cdot\vec{B} - \vec{\mu}_B\cdot\vec{B}$$

$$\mathcal{H}_{ex} = -2\vec{S}_A\cdot\tilde{J}_{AB}\cdot\vec{S}_B \qquad (1)$$

$$\mathcal{H}_{dip} = (\mu_0/4\pi)r_{AB}^{-3}(\vec{\mu}_A\cdot\vec{\mu}_B - 3(\vec{u}_{AB}\cdot\vec{\mu}_A)(\vec{u}_{AB}\cdot\vec{\mu}_B))$$

where

$$\vec{\mu}_A = -\beta\tilde{g}_A\cdot\vec{S}_A, \quad \vec{\mu}_B = -\beta\tilde{g}_B\cdot\vec{S}_B$$

represent the magnetic moments of A and B, respectively. To our knowledge, all studies of magnetic interactions in biological systems have so far been based on this point dipole approximation. However, the structural arrangements predicted by these studies could rarely be compared with those given by independent methods, so the validity of this approximation has not been really assessed. A noteworthy exception was recently provided by the determination of the X-ray crystal structure at 2.4-Å resolution of the enzyme trimethylamine dehydrogenase from the bacterium W_3A_1.[11] This enzyme, which contains a [4Fe–4S] cluster and a flavin group, can be prepared in a state in which the two prosthetic groups are paramagnetic and interact magnetically.[5] Good simulations of EPR spectra recorded at different microwave frequencies were obtained from Hamiltonian 1 by assuming that the dominant term is a ferromagnetic isotropic exchange term ($J_{AB} > 0$) giving a triplet ground state, and the analysis of the dipolar coupling led to a distance r_{AB} in the range 3–5 Å.[5] These conclusions are in serious disagreement with the X-ray crystal structure which indicates that the center-to-center distance between the two prosthetic groups is about 12 Å. Moreover, the long-range superexchange mechanisms are expected to give negative (antiferromagnetic) contributions much smaller in

† Université de Provence.
‡ The University of Sussex.
* Abstract published in *Advance ACS Abstracts*, February 15, 1994.

(1) Lowe, D. J.; Lynden-Bell, R. M.; Bray, R. C. *Biochem. J.* **1972**, *130*, 239–249.
(2) Lowe, D. J.; Bray, R. C. *Biochem. J.* **1978**, *169*, 471–479.
(3) Schepler, K. L.; Dunham, W. R.; Sands, R. H.; Fee, J. A.; Abeles, R. H. *Biochim. Biophys. Acta* **1975**, *397*, 510–518.
(4) Buettner, G. R.; Coffman, R. E. *Biochim. Biophys. Acta* **1977**, *480*, 495–505.
(5) Stevenson, R. C.; Dunham, W. R.; Sands, R. H.; Singer, T. P.; Beinert, H. *Biochim. Biophys. Acta* **1986**, *869*, 81–88.
(6) Dismukes, G. C.; Frank, H. A.; Friesner, R.; Sauer, K. *Biochim. Biophys. Acta* **1984**, *764*, 253–271.
(7) Butler, W. F.; Calvo, R.; Fredkin, D. R.; Isaacson, R. A.; Okamura, M. Y.; Feher, G. *Biophys. J.* **1984**, *45*, 947–973.
(8) Dunham, W. R.; Hagen, W. R.; Fee, J. A.; Sands, R. H.; Dunbar, J. B.; Humblet, C. *Biochim. Biophys. Acta* **1991**, *1079*, 253–262.
(9) Guigliarelli, B.; Guillaussier, J.; More, C.; Setif, P.; Bottin, H.; Bertrand, P. *J. Biol. Chem.* **1993**, *268*, 900–908.
(10) Smith, T. D.; Pilbrow, J. R. *Coord. Chem. Rev.* **1974**, *13*, 173–278.
(11) Lim, L. W.; Shamala, N.; Mathews, F. S.; Steenkamp, D. J.; Hamlin, R.; Xuong, N. *J. Biol. Chem.* **1986**, *261*, 15140–15146.

0002-7863/94/1516-3078$04.50/0

magnitude than the Zeeman energy. The origin of this strong discrepancy is probably due to the failure of the point dipole approximation, which is indeed expected to be very poor in the case of polynuclear clusters and organic radicals in which the magnetic moments are largely delocalized.

In this paper, we examine how the delocalization of the magnetic moments can be taken into account in the description of the magnetic interactions between paramagnetic centers. In the case of organic radicals or mononuclear metal complexes, this delocalization is entirely determined by the spin density distribution and can be easily accounted for by a suitable adaptation of Hamiltonian 1. The situation is completely different for a polynuclear center, in which the delocalization of the magnetic moments is essentially determined by the strong intracluster exchange coupling between different metal sites. For a system containing such polynuclear centers, the magnetic interactions between all the metal sites of the system must then be explicitly considered in the Hamiltonian. Such a *local spin* description is first applied to a system made of a dinuclear center interacting with a mononuclear center and then to a system comprising two interacting dinuclear centers. For these systems, the EPR spectra calculated from the point dipole Hamiltonian 1 and the local spin Hamiltonian are compared for different geometrical configurations. In general, these spectra are different. However, for a large class of geometrical configurations, the spectral shape given by the local spin Hamiltonian can be well reproduced by the point dipole Hamiltonian, provided *effective values* of the parameters r_{AB} and $\tilde{J}_{AB}$ are used in eqs 1. These values may differ strongly from those used in the local spin description, so their structural interpretation is not straightforward. The local spin model has been used to simulate the S-band, X-band, and Q-band EPR spectra of the fully reduced desulfo-inhibited form of the enzyme xanthine oxidase and to determine accurately the relative position of the molybdenum center and of one [2Fe–2S] center (center 1) in this protein.

Materials and Methods

Bovine milk xanthine oxidase was prepared by using selective denaturation with sodium salicylate according to Hart et al.[12] (steps H1 and H2 of Ventom et al.[13]). Desulfo-xanthine oxidase was prepared by treating the enzyme with cyanide.[14] The proportion of functional enzyme remaining was then found to be less than 2% by assays[15] with xanthine. Generation by the original procedure[16] of the desulfo-inhibited Mo(V) species with the iron–sulfur centers reduced frequently yields an EPR spectrum indicating contamination with another Mo(V) species, Slow. Furthermore, extended treatment of concentrated enzyme with ethylene glycol can cause aggregation, leading to EPR line broadening. In this study, the Slow-free desulfo-inhibited signal was obtained by anaerobic dialysis in a glovebox (Faircrest Ltd., U.K.) of the desulfoenzyme (0.35 mL of 0.4 mM) against 100 mL of 50 mM sodium bicine buffer, pH = 8.2, containing 20 mM sodium dithionite and 50% (v/v) ethylene glycol for about 15 h at 20–25 °C. The contents of the dialysis membrane (Medicell, U.K.) were anaerobically transferred to quartz EPR tubes which were stoppered with Suba-Seals, removed from the glovebox, and immediately frozen in liquid nitrogen.

X-band spectra were recorded on a Bruker ESP 300 spectrometer equipped with the ESP 1620 data processing unit. Q-band spectra were recorded on a Varian E112 spectrometer equipped with a Varian E110 microwave bridge. The samples were cooled by an Oxford Instruments ESR 900 cryostat at X-band and by an Air-Products Helitran gas-flow system at Q-band. Before and after the recording of each spectrum, the temperature was measured with a calibrated thermocouple (chromel vs Au/0.07% Fe) placed in an EPR tube partially filled with water. S-band spectra were recorded on a Bruker ESP 300 spectrometer equipped with an ER 061 SR microwave bridge and fitted with a CF 935 Oxford cryostat.

Spectral simulations based on the point dipole Hamiltonian 1 were performed according to the procedure previously applied to centers A and B of photosystem I[9] (program POINTDIP). Spectral simulations based on the local spin Hamiltonian 4 were performed by the program DIPLOC. This program was written to diagonalize numerically this Hamiltonian and to calculate the position and the transition probability of the resonance lines in the case of two centers with $S = {}^1/_2$. In both of these programs, the line widths are assumed to originate essentially from strain effects, which are treated by an elaborate procedure which is outlined below. All the parameters p_i describing the magnetic characteristics and the geometrical configuration of the system are considered as random variables characterized by their mean values $p_i°$, their standard deviations σ_i, and the correlation coefficients c_{ij}. For a given orientation of the magnetic field, the energy E_k of an EPR transition is then a random variable whose mean value $E_k°$ and standard deviation Σ_k can be expressed in terms of the $p_i°$, σ_i, and c_{ij} and of the partial derivatives $\partial E_k/\partial p_i$ and $\partial^2 E_k/\partial p_i^2$. The resulting line shape is assumed to be Gaussian in energy. This statistical procedure was first introduced by Hagen et al.[17] to describe the *g*-strain effect in metalloproteins. In that case, the partial derivatives could be expressed in closed form.[17] Owing to the complexity of the Hamiltonian, this is no longer possible in the case of a system made of several interacting centers, for which all partial derivatives have to be evaluated numerically. In practice, good simulations were achieved by assuming that a limited number of parameters were distributed.

All numerical simulations were performed on a 3090 IBM computer, with typical CPU times of about 100 s.

Dipolar Interactions between Delocalized Magnetic Moments

Consider two centers A and B in which the magnetic moments $\vec{\mu}_A$ and $\vec{\mu}_B$ result from the addition of point dipoles $\vec{\mu}_{Ai}$ and $\vec{\mu}_{Bj}$:

$$\vec{\mu}_A = \sum_i \vec{\mu}_{Ai} \qquad \vec{\mu}_B = \sum_j \vec{\mu}_{Bj}$$

The Hamiltonian describing the dipolar interactions between A and B is written:

$$\mathcal{H}_{dip} = (\mu_0/4\pi)\sum_{ij} r_{ij}^{-3}(\vec{\mu}_{Ai}\cdot\vec{\mu}_{Bj} - 3(\vec{u}_{ij}\cdot\vec{\mu}_{Ai})(\vec{u}_{ij}\cdot\vec{\mu}_{Bj})) \quad (2)$$

where r_{ij} is the distance between the point dipoles $\vec{\mu}_{Ai}$ and $\vec{\mu}_{Bj}$ and $\vec{u}_{ij}$ is a unit vector along the line joining the two dipoles. The extension to a continuous distribution of magnetic dipoles is straightforward. Although eq 12 is general, the expression of the magnetic moments $\vec{\mu}_{Ai}$ and $\vec{\mu}_{Bj}$ depends on the nature of the centers. For an organic radical or a mononuclear metal complex, the delocalization of the magnetic electrons is well described in terms of molecular orbitals extending over the whole paramagnetic center. In this case, the center is characterized by a unique *g* tensor, and the delocalization of the magnetic moment is entirely determined by the spin density distribution: if atom *i* of center A carries a spin density ρ_{Ai}, it carries a local magnetic moment $\vec{\mu}_{Ai} = \rho_{Ai}\vec{\mu}_A$. Equation 2 then reduces to:

$$\mathcal{H}_{dip} = (\mu_0/4\pi)\sum_{ij} r_{ij}^{-3}\rho_{Ai}\rho_{Bj}(\vec{\mu}_A\cdot\vec{\mu}_B - 3(\vec{u}_{ij}\cdot\vec{\mu}_A)(\vec{u}_{ij}\cdot\vec{\mu}_B)) \quad (3)$$

where the sum is performed over all atoms *i* and *j* of centers A and B, respectively. The use of eq 3 appears especially necessary for organic radicals, in which the spin density is generally largely delocalized.[18] In the case of mononuclear metal complexes, the spin density is essentially localized on the metal ion. The dipolar interactions between two such centers are then expected to be well described by the point dipole model (eq 1), provided $\vec{u}_{AB}$ and r_{AB} refer to the vector joining the metal ions. Detailed calculations have shown that for such mononuclear metal complexes, the point dipole description remains a good approximation even for very short metal-to-metal distances. For example, in the system $(VF_5)^{3-}$–F^-–$(VF_5)^{3-}$ in $KMgF_3$, the two $S = {}^3/_2$ V^{2+} ions are separated by only 4 Å and are coupled by strong antiferromagnetic

(12) Hart, L. I.; McGartoll, M. A.; Chapman, H. R.; Bray, R. C. *Biochem. J.* **1970**, *116*, 851–864.
(13) Ventom, A. M.; Deistung, J.; Bray, R. C. *Biochem. J.* **1988**, *255*, 949–956.
(14) Massey, V.; Edmonson, D. *J. Biol. Chem.* **1970**, *245*, 6595–6598.
(15) Bray, R. C. In *The Enzymes*, 3rd ed.; Boyer, P. D., Ed.; Academic Press: New York, 1975; Vol. 12, pp 299–419.
(16) Lowe, D. J.; Barber, M. J.; Pawlik, R. T.; Bray, R. C. *Biochem. J.* **1976**, *155*, 81–85.
(17) Hagen, W. R.; Hearshen, D. O.; Sands, R. H.; Dunham, W. R. *J. Magn. Reson.* **1985**, *61*, 220–232.
(18) Bencini, A.; Gatteschi, D. *EPR of Exchange Coupled Systems*; Springer: Berlin, 1990.

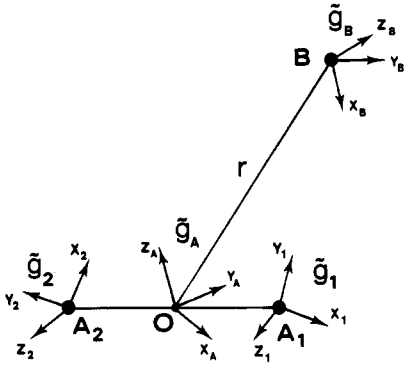

Figure 1. Different g tensors used in a local spin description of the magnetic interactions between a dinuclear center A and a mononuclear center B.

exchange interactions, giving an $S = 0$ ground state.[19] In the $S = 2$ excited state, the dipolar terms appear as a contribution to the zero-field splitting tensor. When this contribution is calculated from the point dipole Hamiltonian 1 and the more accurate Hamiltonian 3, it turns out that the results differ by only 20%.[19]

The situation is different when at least one center is a polynuclear metal cluster. The numerous experimental and theoretical studies that have been devoted to these clusters have demonstrated that their electronic structure is best described in terms of valence bond models.[18,20] In the spin Hamiltonian formalism, each metal site is then characterized by *local* spin Hamiltonian parameters, like the g, hyperfine, and zero-field splitting tensors, and the physical observables of the cluster are expressed in terms of these local parameters by standard angular momentum algebra. The dipolar interactions between two such clusters A and B must then be written according to eq 2, in which the magnetic moments can be considered as centered on the metal ions. In the following, this *local spin* model is developed and compared to the point dipole model.

Magnetic Interactions between a Dinuclear Center and a Mononuclear Center

Consider a paramagnetic dinuclear center A comprising two exchange-coupled metal sites A_1 and A_2. In the case of known biological dinuclear clusters, the valences are trapped, so that A_1 and A_2 can be characterized by well-defined values of their spin and g tensor, which are noted $S_1,\tilde{g}_1$ and $S_2,\tilde{g}_2$, respectively. These two sites are interacting with a mononuclear center characterized by $S_B,\tilde{g}_B$ (Figure 1). In the presence of an applied field, the spin Hamiltonian describing this system is given by $\mathcal{H} = \mathcal{H}_0 + \mathcal{H}_{int}$, where $\mathcal{H}_0$ includes the internal coupling between A_1 and A_2, and $\mathcal{H}_{int}$ is expressed as:

$$\mathcal{H}_{int} = \mathcal{H}_z + \mathcal{H}_{ex} + \mathcal{H}_{dip}$$

$$\mathcal{H}_z = -\vec{\mu}_1\cdot\vec{B} - \vec{\mu}_2\cdot\vec{B} - \vec{\mu}_B\cdot\vec{B}$$

$$\mathcal{H}_{ex} = -2\vec{S}_1\cdot\tilde{J}_{1B}\cdot\vec{S}_B - 2\vec{S}_2\cdot\tilde{J}_{2B}\cdot\vec{S}_B \qquad (4)$$

$$\mathcal{H}_{dip} = (\mu_0/4\pi)\sum_{i=1,2} r_{iB}^{-3}(\vec{\mu}_i\cdot\vec{\mu}_B - 3(\vec{u}_{iB}\cdot\vec{\mu}_i)(\vec{u}_{iB}\cdot\vec{\mu}_B))$$

with

$$\vec{\mu}_k = -\beta\tilde{g}_k\cdot\vec{S}_k, \quad k = 1, 2, B$$

For the dinuclear clusters found in biological molecules, the ground multiplet is generally well separated from the excited states and can be labeled with a particular value $S_{12}°$ of the total spin $\vec{S}_{12} = \vec{S}_1 + \vec{S}_2$. In the following, we consider the usual situation in which the magnitude of the intercenter magnetic interactions is much smaller than the intracenter exchange coupling. In these conditions, the diagonalization of Hamiltonian 4 can be restricted to the subspace $\{|S_{12}°,M_{12}\rangle|S_B,M_B\rangle\}$. According to the Wigner–Eckart theorem, $\vec{S}_1$ and $\vec{S}_2$ can then be substituted in eqs 4 by $K_1\cdot\vec{S}_{12}$ and $K_2\cdot\vec{S}_{12}$, respectively, with:[18]

$$K_1 = (S_{12}°(S_{12}° + 1) + S_1(S_1+1) - S_2(S_2+1))/(2S_{12}°(S_{12}° + 1)) \qquad (5)$$

and a symmetrical expression for K_2. The Zeeman and exchange terms of Hamiltonian 4 are then equivalent to those of the point dipole Hamiltonian 1 provided that:

$$\vec{S}_A = \vec{S}_{12}$$

$$\tilde{g}_A = K_1\tilde{g}_1 + K_2\tilde{g}_2 \qquad (6)$$

$$\tilde{J}_{AB} = K_1\tilde{J}_{1B} + K_2\tilde{J}_{2B} \qquad (7)$$

Expression 6 is well known. In this context, it recalls only the physical origin of the $\tilde{g}_A$ components, which can generally be directly measured experimentally. Expression 7 is similar and shows that the parameter $\tilde{J}_{AB}$ to be used in an equivalent point dipole spin Hamiltonian is in fact an *effective* parameter whose value depends not only on $\tilde{J}_{1B}$ and $\tilde{J}_{2B}$ but also on the electronic structure of the dinuclear center A through the weighting coefficients K_1 and K_2. This important point can be illustrated by considering the case of a $[2Fe–2S]^+$ cluster interacting with a mononuclear center. The strong antiferromagnetic coupling between the Fe(III) site with $S_1 = {}^5/_2$ and the Fe(II) site with $S_2 = 2$ leads to a ground state with $S_{12}° = {}^1/_2$, for which $K_1 = {}^7/_3$ and $K_2 = -{}^4/_3$. The dominant contribution to long-range intercenter exchange interactions is probably an isotropic superexchange term which is antiferromagnetic, so that J_{1B} and J_{2B} are expected to be both negative. However, the effective parameter J_{AB} given by

$$J_{AB} = {}^7/_3J_{1B} - {}^4/_3J_{2B} \qquad (8)$$

can be either positive or negative, depending on the relative efficiency of the superexchange pathways which determine J_{1B} and J_{2B}. The two limiting situations are schematically represented in Figure 2.

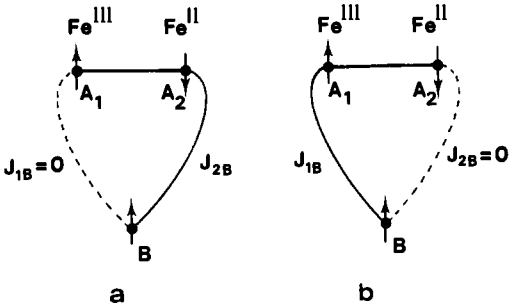

Figure 2. Schematic representation of the two limiting cases corresponding to eq 8 for an [Fe(III),Fe(II)] cluster coupled by long-range antiferromagnetic exchange interactions to a mononuclear center B. In case a, $J_{AB} = -{}^4/_3J_{2B}$ is positive, whereas in case b, $J_{AB} = {}^7/_3J_{1B}$ is negative.

We now consider the dipolar interactions. In general, the dipolar terms of Hamiltonian 4 cannot be replaced by an equivalent point dipole term in the same straightforward way as the Zeeman and exchange terms. In the following, we examine if the effects of these dipolar terms can nevertheless be described by an approximate point dipole treatment.

In fact, there is one particular situation in which these terms are exactly equivalent to a point dipole counterpart, namely when the g tensors of sites A_1 and A_2 are identical, $\tilde{g}_1 = \tilde{g}_2 = \tilde{g}_A$, and A_1, A_2, and B are collinear, $\vec{u}_{1B} = \vec{u}_{2B} = \vec{u}_{AB}$. In this case, it is easy to verify that the dipolar terms of Hamiltonian 4 reduce to those of Hamiltonian 1 provided that r_{AB} is given by:

(19) Smith, S. R. P.; Owen, J. *J. Phys. C: Solid State Phys.* **1971**, *4*, 1399–1408.

(20) Noodleman, L.; Case, D. A. *Adv. Inorg. Chem.* **1992**, *38*, 423–470.

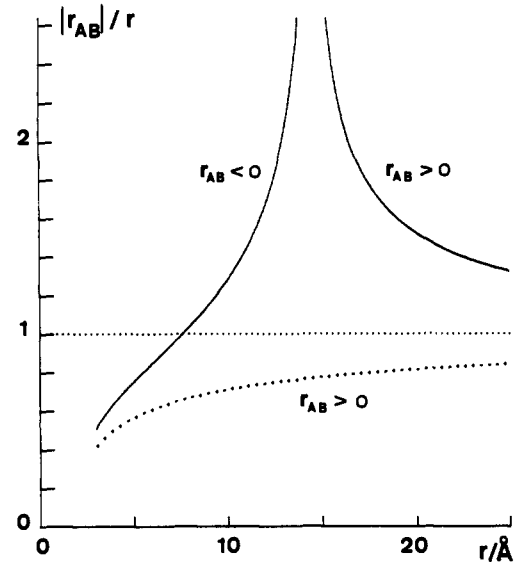

Figure 3. Variations of the effective distance r_{AB} defined by eq 9 as a function of r, for the two collinear configurations of a system comprising an [Fe(III),Fe(II)] cluster coupled to a mononuclear center B. (—) Fe(III)—Fe(II)···B configuration; (- - -) Fe(II)—Fe(III)···B configuration.

$$r_{AB}^{-3} = K_1 r_{1B}^{-3} + K_2 r_{2B}^{-3} \tag{9}$$

It is interesting to compare this *effective distance* r_{AB} to the geometrical distance r defined in Figure 1 in the typical case of a [2Fe–2S]$^+$ cluster in which the iron-to-iron distance is 2.7 Å. We have represented in Figure 3 the variations of r_{AB} as a function of r for the two possible collinear configurations of the system. When center B is on the side of the ferric ion, r_{AB} is positive but remains significantly smaller than r. When center B is on the side of the ferrous ion, r_{AB} may be either positive or negative. Its magnitude may depart notably from r and becomes even infinite for $r \simeq 14.5$ Å. In these peculiar circumstances, the dipolar interactions vanish exactly, so that this distance can be called a "magic distance".

These results concern particular collinear configurations of the system, and it is important to examine if similar effects are observed in more general situations.

EPR spectra were then calculated with the program DIPLOC on the basis of the local spin Hamiltonian 4 for the following system: the three g tensors were assumed isotropic with $g_1 = g_2 = g_B = 2.00$ and $S_1 = {}^5/_2$, $S_2 = 2$. The exchange interactions between A and B were set equal to zero. Because of the isotropy of the g tensors, the geometry is defined only by the distance $r = |\overrightarrow{OB}|$ and the angle $\theta = (\overrightarrow{A_2A_1},\overrightarrow{OB})$. The distance A_1A_2 was set equal to 2.7 Å as in a [2Fe–2S]$^+$ cluster. The resonance lines were taken as Gaussian with a small peak-to-peak line width in order to show the spectral shape variations.

The calculated spectra are represented in Figure 4 for r = 17, 13, 10, and 7 Å and different values of θ (45°, 90°, 135°). We recall that the values $\theta = 0°$ and $\theta = 180°$ correspond to the two collinear arrangements. We observe that for a fixed distance r, the spectra are strongly dependent on θ (Figure 4). This angular dependence is, of course, not predicted by Hamiltonian 1 based on the point dipole model. However, we know that Hamiltonian 1 is exactly equivalent to Hamiltonian 4 when $\theta = 0°$ and $\theta = 180°$ if r_{AB} is taken equal to the value given by eq 9. This suggests that this equation may provide a simple way to account for the angular dependence through the point dipole approximation. We have shown in Figure 4 the spectra calculated with the program POINTDIP using the value of r_{AB} calculated by eq 9 as a function of r and θ. For a fixed distance r, the effective distance r_{AB} depends strongly on θ and is close to r only for $\theta = 90°$. For large values of r, the spectra computed from the point dipole model are similar to those given by the local spin model. However, the effective distance calculated from eq 9 is not always the best value required to reproduce the spectral shape given by the local spin description. This is especially true for large values of θ ($\theta = 90°, 135°$), where the differences between the spectra calculated from the point dipole and local spin models increase rapidly as r decreases (Figure 4b,c). At short center-to-center distances, the local spin description leads to new spectral shapes that cannot be reproduced by the point dipole approximation (Figure 4d).

The conclusion one may draw from all these observations is that spectral simulations based on Hamiltonian 1 are similar to those based on the local spin model when the distance r is not too short. In this case the phenomenological parameter r_{AB} of the point dipole approximation is not very different from the effective distance given by eq 9 when the mononuclear center B is on the ferric ion side of the dinuclear complex A but departs markedly from this value as B approaches the ferrous ion side. Nevertheless, this effective distance appears as a valuable tool to start a fitting procedure based on Hamiltonian 4. Another remark is that the similarity between spectra given by the two simulation procedures would, of course, be observed over a wider range of geometrical configurations if the line widths were broader than the very narrow ones used in Figure 4.

All the peculiar effects encountered in this section are due to the delocalization o the magnetic moment over the two metal sites of the dinuclear cluster and vanish when the distance between A_1 and A_2 is set equal to zero. Similar effects occur in the case of two interacting polynuclear clusters. This is illustrated below by the simple case of two dinuclear centers.

Magnetic Interactions between Two Dinuclear Centers

We now consider a system comprising two interacting dinuclear centers A and B. Cluster A is made of two coupled metal sites A_1 and A_2 with spins S_1 and S_2, and cluster B is made of two coupled sites B_3 and B_4 with spins S_3 and S_4. In the presence of an applied field, the spin Hamiltonian describing the intercenter magnetic interactions is given by the following set of equations:

$$\mathcal{H}_{int} = \mathcal{H}_z + \mathcal{H}_{ex} + \mathcal{H}_{dip}$$

$$\mathcal{H}_z = \sum_{i=1}^{4} -\vec{\mu}_i \cdot \vec{B}$$

$$\mathcal{H}_{ex} = \sum_{i=1}^{2}\sum_{j=3}^{4} -2\vec{S}_i \cdot \tilde{J}_{ij} \cdot \vec{S}_j \tag{10}$$

$$\mathcal{H}_{dip} = (\mu_0/4\pi)\sum_{i=1}^{2}\sum_{j=3}^{4} r_{ij}^{-3}(\vec{\mu}_i \cdot \vec{\mu}_j - 3(\vec{u}_{ij} \cdot \vec{\mu}_i)(\vec{u}_{ij} \cdot \vec{\mu}_j))$$

with

$$\vec{\mu}_k = -\beta \tilde{g}_k \cdot \vec{S}_k, \quad k = 1, 2, 3, 4$$

As in the preceding section, we consider the usual situation in which the ground state of each dinuclear cluster is well isolated from excited states and can be labeled by a value of the total spin $S_{12}°$ and $S_{34}°$ for A and B, respectively. The diagonalization of Hamiltonian 10 can then be performed in the subspace $\{|S_{12}°, M_{12}\rangle|S_{34}°, M_{34}\rangle\}$, in which the Zeeman and exchange terms are equivalent to those of the point dipole Hamiltonian 1, provided that:

$$\vec{S}_A = \vec{S}_{12} \qquad \vec{S}_B = \vec{S}_{34}$$

$$\tilde{g}_A = K_1\tilde{g}_1 + K_2\tilde{g}_2 \qquad \tilde{g}_B = K_3\tilde{g}_3 + K_4\tilde{g}_4$$

$$\tilde{J}_{AB} = \sum_{ij} K_i K_j \tilde{J}_{ij} \qquad i = 1, 2; \; j = 3, 4 \tag{11}$$

The weighting coefficients K_i are given by expressions similar to

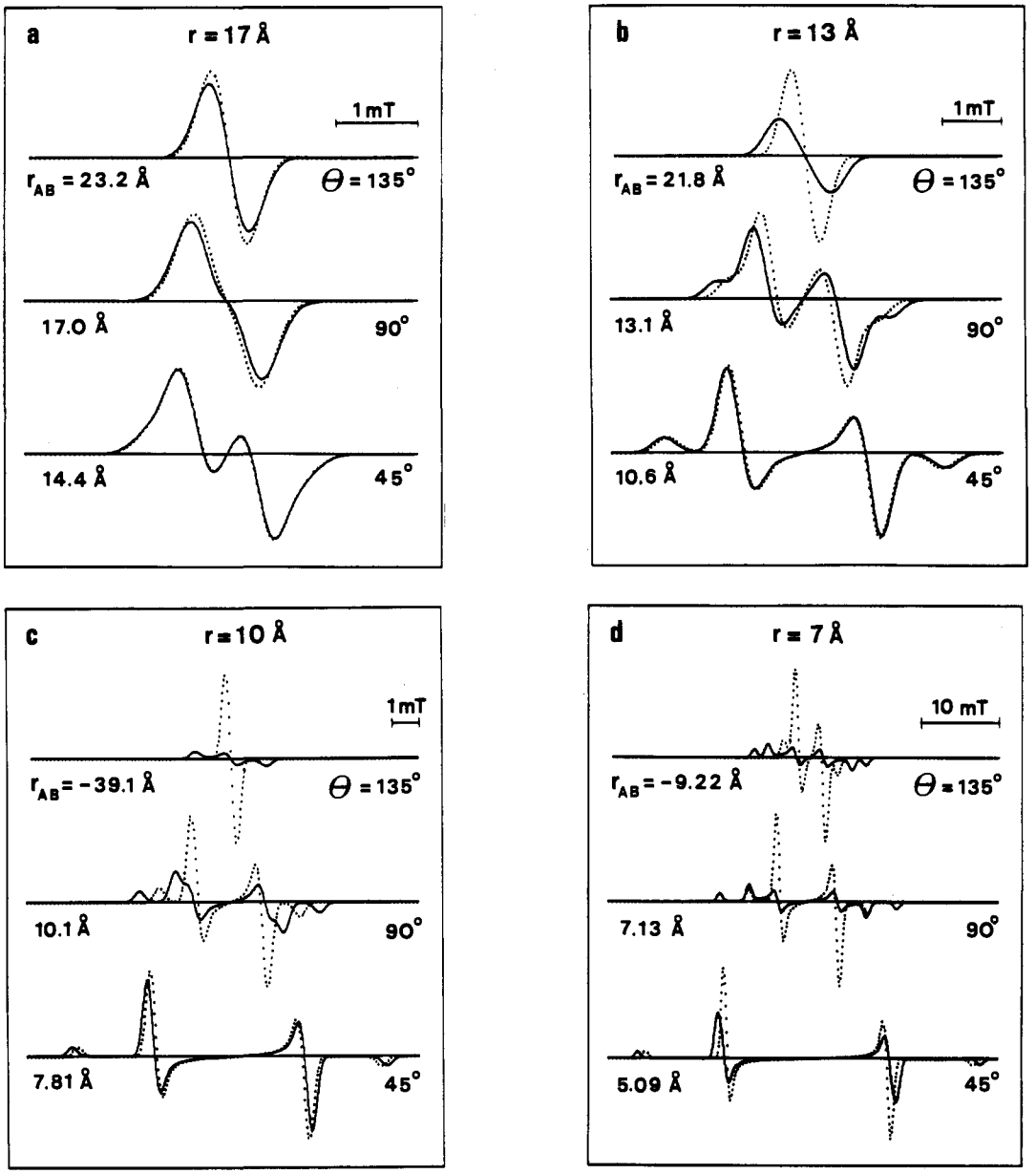

Figure 4. Comparison of EPR spectra calculated from the point dipole and local spin models for a system made of an [Fe(III),Fe(II)] cluster coupled by dipolar interactions to a mononuclear center B, in the case $g_1 = g_2 = g_B = 2.00$. r is the center-to-center distance, and θ the angle between $\overrightarrow{A_2A_1}$ and OB. (—) Spectra computed from the local spin Hamiltonian 4; (- - -) spectra computed from the point dipole Hamiltonian 1 with the value of r_{AB} given by eq 9. For a given set (r,θ), the spectra are normalized in intensity. The microwave frequency used in the calculation was 9258 MHz. The peak-to-peak line width was taken equal to 0.4 mT in a, b, and c and 0.8 mT in d.

eq 5. Expression 11 shows that the parameter $\tilde{J}_{AB}$ is an *effective* parameter whose magnitude and sign depend not only on all the exchange interactions between the different subunits of the system but also on the electronic states of both clusters. This can be illustrated by the example of a Mn(IV)–Mn(III) cluster in which the strong intracluster antiferromagnetic coupling between the Mn(IV) ($S_1 = {}^3/_2$) and Mn(III) ($S_2 = 2$) sites gives rise to a ground state with $S_{12}° = {}^1/_2$. We assume that these sites are coupled by weak antiferromagnetic interactions to the Mn(IV) ($S_3 = {}^3/_2$) and Mn(III) ($S_4 = 2$) sites of a similar cluster (Figure 5). For this system, $K_1 = K_3 = -1$ and $K_2 = K_4 = 2$ so that expression 11 predicts $J_{AB} = J_{13} + 4J_{24} < 0$ in situation a of Figure 5 and $J_{AB} = -2J_{14} - 2J_{23} > 0$ in situation b. It is interesting to note that situation b is apparently observed in $(Mn_2O_2)_2$-$(tphpn)_2(ClO_4)_4$, a dimer of di-μ-oxo dimers that mimics the S_1 state of the photosystem II manganese aggregate.[21] Examination of the X-ray crystal structure of this compound reveals the existence of trapped valence sites organized according to Figure 5b and suggests that the interdimer exchange interactions described by J_{14} and J_{23} are much weaker than the intradimer coupling. A positive value is then anticipated for the effective exchange parameter J_{AB}. This was recently confirmed by a magnetic susceptibility study which demonstrated that the ground state of the system is a spin triplet.[22] A complete quantitative analysis of the magnetic interactions within this system is developed in ref 22.

Another example is given by a system comprising two [2Fe–2S]$^+$ clusters, in which the long-range interactions between iron sites belonging to different clusters are antiferromagnetic: when these interactions take place between iron sites with the same valences, the effective exchange parameter $J_{AB} = (49/9)J_{13} + (16/9)J_{24}$ is negative, whereas when they take place between iron sites possessing different valencies, $J_{AB} = (-28/9)J_{14} - (28/9)J_{23}$

(21) Chan, M. K.; Armstrong, W. H. *J. Am. Chem. Soc.* **1991**, *113*, 5055–5057.

(22) Kirk, M. L.; Chan, M. K.; Armstrong, W. H.; Solomon, E. I. *J. Am. Chem. Soc.* **1992**, *114*, 10432–10440.

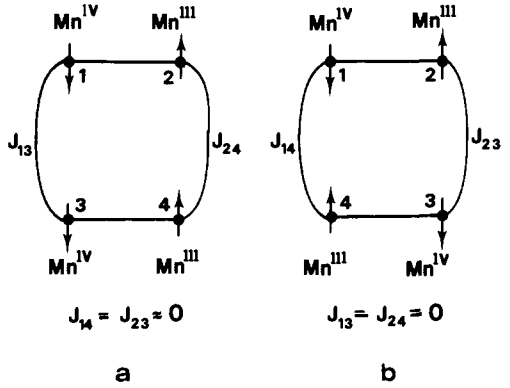

Figure 5. Schematic representation of the two limiting cases corresponding to eq 11 for two [Mn(IV),Mn(III)] clusters coupled by long-range antiferromagnetic interactions. In case a, $J_{AB} = J_{13} + 4J_{24}$ is negative, whereas in case b, $J_{AB} = -2J_{14} - 2J_{23}$ is positive.

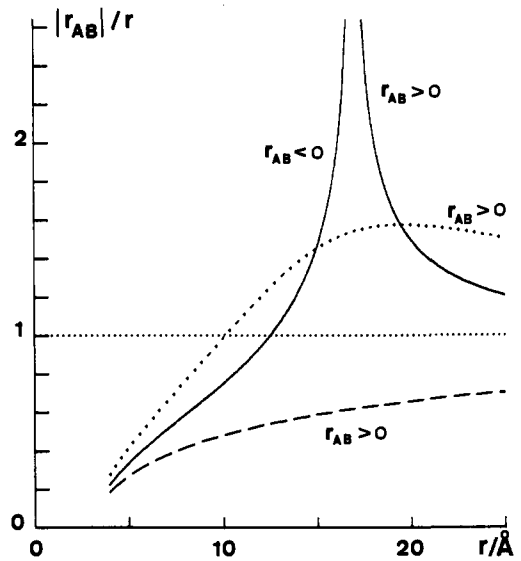

Figure 6. Variations of the effective distance r_{AB} given by expression 12 for the three possible linear arrangements of a system made of two [Fe(III),Fe(II)] dinuclear centers. (—) Fe(II)—Fe(III)···Fe(II)—Fe(III) configuration; (- - -) Fe(III)—Fe(II)···Fe(II)—Fe(III) configuration; (– – –) Fe(II)—Fe(III)···Fe(III)—Fe(II) configuration.

is positive. In these equations, subscripts 1 and 3 refer to the ferric sites and 2 and 4 to the ferrous sites.

We now consider the dipolar terms of Hamiltonian 10. These terms reduce to those of the point dipole Hamiltonian 1 only when the g tensors of sites A_1 and A_2 on the one hand and of sites B_3 and B_4 on the other hand are equal, $\tilde{g}_1 = \tilde{g}_2 = \tilde{g}_A$, $\tilde{g}_3 = \tilde{g}_4 = \tilde{g}_B$, and the four metal ions are collinear, provided that the effective distance r_{AB} is given by

$$r_{AB}^{-3} = \sum_{i,j} K_i K_j r_{ij}^{-3} \qquad i = 1, 2;\ j = 3, 4 \qquad (12)$$

The variations of r_{AB} upon the center-to-center distance r are illustrated in Figure 6 in the case of two interacting [2Fe–2S]$^+$ clusters for the three possible configurations of the system. Here again, r_{AB} may be either positive or negative, and in general its magnitude departs markedly from r. These effects, which proceed from the spin-coupled structure of the dinuclear clusters, are not restricted to the collinear arrangement. By analogy with the case treated in the preceding section, they are expected to occur in a wide range of geometrical configurations. However, numerous parameters are necessary to define the geometrical arrangement of two dinuclear clusters in the most general situation. For that reason, and also because we are not aware of any example of dinuclear clusters coupled by weak magnetic interactions in biological systems, we have not attempted to study systematically how r_{AB} depends on the geometry of the system.

Study of the Magnetic Interactions between the [2Fe–2S] Center 1 and the Molybdenum Center in the Enzyme Xanthine Oxidase

Milk xanthine oxidase is a molybdoflavoenzyme containing one molybdenum center, one FAD, and two [2Fe–2S] clusters in each of its two catalytically independent subunits.[1,15] In the fully reduced state, this protein exhibits at low temperature a complex EPR spectrum arising from the contributions of the Mo(V) and the [2Fe–2S]$^+$ centers. At temperatures higher than about 35 K, the signal of one [2Fe–2S]$^+$ center, center 2, disappears due to its very fast spin–lattice relaxation properties and a spectrum manifesting magnetic interactions between the Mo(V) center and the other [2Fe–2S] center, center 1, is observed.[1] This spectrum, which provided one of the first examples for the existence of intercenter magnetic interactions in biological molecules, has been extensively studied at X-band and Q-band for different ligation states of the molybdenum center.[1,2] Different semiquantitative interpretations of these spectra have been proposed, yielding estimates of the intercenter distance in the range 20–25 Å,[2] 8–14 Å,[23] and > 15 Å,[24] but no spectral simulation has so far been presented in the literature. The dynamic effects of the magnetic interactions in xanthine oxidase were also studied by Barber et al.[25] These authors put in evidence a strong shortening of the spin–lattice relaxation time of the Mo(V) center induced by the magnetic coupling with center 1 but did not succeed in separating the exchange and dipolar contributions.

We have used the local spin model presented above to study quantitatively the magnetic interactions between the Mo(V) center and center 1 in xanthine oxidase. This is most conveniently done by using the desulfo-inhibited form of the enzyme, in which the Mo(V) signal is very sharp and uncomplicated by resolved hyperfine interactions with protons.[2] The pure Mo(V) signal can be observed at high temperature, where the signal of center 1 has disappeared due to relaxation broadening (Figure 7). The shape of this signal is strongly frequency dependent, which indicates that the line widths contain an important contribution from unresolved hyperfine interactions with neighboring paramagnetic nuclei. The X-band and Q-band spectra exhibit weak amplitude hyperfine lines arising from about 25% of molecules in which the molybdenum nuclei carry an $I = {}^5/_2$ spin. In the following, we shall ignore the contribution of these molecules and concentrate on the main part of the spectrum, which is given by Mo(V) centers with $I = 0$. The broadening mechanisms responsible for the line widths of these high-temperature spectra also contribute to the line widths of the low-temperature interaction spectra. We have attempted to include in an empirical way these different mechanisms in our simulations by resorting to a simple g-strain procedure: the high-temperature spectra were simulated by the program POINTDIP, by considering the special case of two noninteracting identical centers ($r_{AB} = \infty$, $J_{AB} = 0$). In this limit, our line width treatment reduces to that described in ref 17: the distribution of the g tensor around a mean tensor $\tilde{g}_0$ is described by a three-dimensional tensor $\tilde{p}$ whose principal elements are random variables p_i characterized by their standard deviations σ_i. Good simulations were achieved by assuming that $\tilde{g}_0$ and $\tilde{p}$ are collinear and by taking the random variables to be fully positively correlated and frequency dependent (Figure 7). When expressed in magnetic field units, the effective line widths obtained in this way first decrease and then increase again when the frequency increases. This "anomalous" variation can be explained as follows: the hyperfine lines due to molybdenum nuclei, which are resolved at Q-band and even at X-band, are ignored in our simulations (Figure 7b and c). At S-band,

(23) Coffman, R. E.; Buettner, G. R. *J. Phys. Chem.* **1979**, *83*, 2392–2400.
(24) George, G. N. In *Flavins and Flavoproteins*; Bray, R. C., Engel, P. C., Mahyew, S. C., Eds.; de Gruyter: Berlin, 1984; pp 325–330.
(25) Barber, M. J.; Salerno, J. C.; Siegel, L. M. *Biochemistry* **1982**, *21*, 1648–1656.

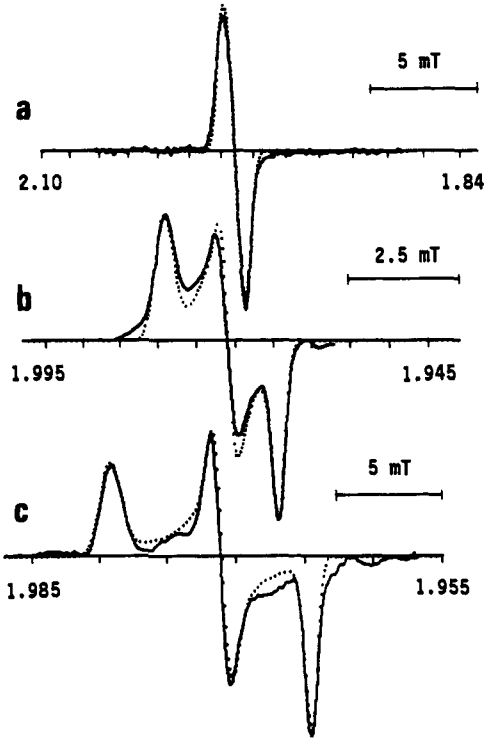

Figure 7. High-temperature Mo(V) EPR spectra of the desulfo-inhibited form of milk xanthine oxidase with iron–sulfur centers fully reduced. (—) Experimental spectra: (a) S-band, microwave frequency 4041.17 MHz, power 0.2 mW, temperature 140 K, modulation amplitude 0.2 mT; (b) X-band, microwave frequency 9337.18 MHz, power 1.0 mW, temperature 200 K, modulation amplitude 0.2 mT; (c) Q-band, microwave frequency 35 052 MHz, power 0.5 mW, temperature 130 K, modulation amplitude 0.25 mT. (···) Best simulations given by the program POINTDIP with the following parameters: $g_{x,y,z} = 1.9646, 1.9710, 1.9792$; line widths (in unit of 10^{-4}), S-band, $\sigma_{x,y,z} = 38, 36, 32$; X-band, $\sigma_{x,y,z} = 8, 13, 12$; Q-band, $\sigma_{x,y,z} = 4.8, 5.2, 8$.

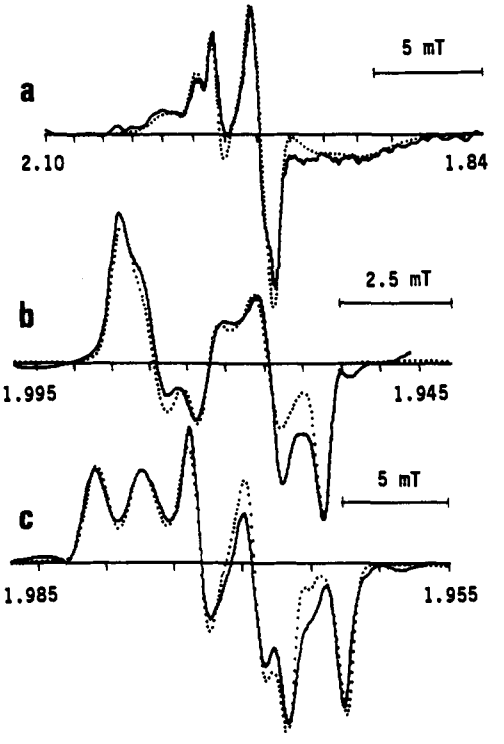

Figure 8. Low-temperature Mo(V) EPR spectra of the desulfo-inhibited form of milk xanthine oxidase with iron–sulfur centers fully reduced. (sbd) Experimental spectra: (a) S-band, microwave frequency 4040.3 MHz, power 0.02 mW, temperature 40 K, modulation amplitude 1.0 mT; (b) X-band, microwave frequency 9399.39 MHz, power 0.1 mW, temperature 40 K, modulation amplitude 0.1 mT; (c) Q-band, microwave frequency 35 105 MHz, power 0.05 mW, temperature 36 K, modulation amplitude 0.25 mT. (···) Best simulations given by the local spin model, with the structural parameters reported in Table 1 and the following g tensor characteristics: Mo(V) center, same as in Figure 7; Fe(III) center, $g_{1x,y,z} = 2.015, 2.034, 2.030$; Fe(II) center, $g_{2x,y,z} = 2.106, 2.110, 2.036$. The S-band spectrum was interpreted as the superimposition of a component arising from molecules in which the molybdenum atoms are paramagnetic and a component arising from molecules giving a pure center 1 signal.

these lines are no longer resolved, and their effect is included in the effective line width needed to fit the experimental spectrum (figure 7a).

At low temperature, the magnetic interactions with center 1 give rise to a complex frequency-dependent pattern of lines in the Mo(V) part of the spectrum (Figure 8), whereas the signal of center 1 is only broadened at X-band and Q-band[2] and also at S-band (Figure 8). This is due to the much larger line width of this signal and also to the fact that the redox state of the sample is such that all the molybdenum atoms are not present as Mo(V),[2] so that only a fraction of centers 1 experience the magnetic interactions. In the following, we focus our attention to the Mo(V) region of the spectrum and consider the effect of the magnetic interactions on center 1 only at S-band, where their effect is maximum.

The program DIPLOC has been written to perform numerical spectral simulations based on Hamiltonian 4 in the case $S_1 = {}^5/_2$, $S_2 = 2$, and $S_{12}{}^o = S_B = {}^1/_2$. The geometry of the system (A_1A_2B) is defined as follows: let (x_1,y_1,z_1), (x_2,y_2,z_2), and (x_B,y_B,z_B) be the principal axes of $\tilde{g}_1$, $\tilde{g}_2$ and $\tilde{g}_B$, respectively. The orientation of $\overrightarrow{A_1A_2}$ and the position of center B are defined in the axes system (x_A,y_A,z_A) centered at 0, midpoint of A_1A_2, in which the resulting $\tilde{g}_A$ tensor defined by eq 6 is diagonal (Figure 1). The orientation of (x_B,y_B,z_B) with respect to (x_A,y_A,z_A) is defined by a set of Euler angles. In order to use this program, it is first necessary to define the local g tensors of the ferric and ferrous sites which yield the resulting tensor $\tilde{g}_A$ of the doublet ground state of the [2Fe–2S] center 1. This can be done by resorting to the ligand field model which accounts for the magnetic properties of $[2Fe–2S]^+$ centers with $g_{av} = 1.96$ in metalloproteins.[26,27] In this model, an idealized C_{2v} symmetry is assumed

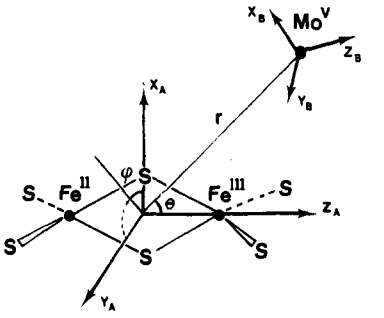

Figure 9. Structural model used to describe the magnetic interactions between the Mo(V) center and iron–sulfur center 1 in xanthine oxidase.

for each metal site, so that $\tilde{g}_1$, $\tilde{g}_2$, and the resulting tensor $\tilde{g}_A$ have their magnetic axes parallel and oriented according to Figure 9. Within the $g_{av} = 1.96$ class, the components of the ferric g tensor are approximately constant and equal to $g_{1x} = 2.015$, $g_{1y} = 2.034$, $g_{1z} = 2.030$. The g values of center 1, $g_x = 1.894$, $g_y = 1.932$, $g_z = 2.022$,[28] $g_{av} = 1.95$, are close to those of some $[2Fe–2S]^+$ centers of the $g_{av} = 1.96$ class, so that the g tensors are expected to be well described by the same ligand field model. The geometry of the system is then defined according to Figure 9, the position

(26) Bertrand, P.; Gayda, J. P. *Biochim. Biophys. Acta* **1979**, *579*, 107–121.
(27) Bertrand, P.; Guigliarelli, B.; More, C. *New J. Chem.* **1991**, *15*, 445–454.
(28) Hille, R.; Hagen, W. R.; Dunham, W. R. *J. Biol. Chem.* **1985**, *260*, 10569–10575.

Table 1. Structural Parameter Values Used in the Best Simulations of the Low-Temperature Spectra of Xanthine Oxidase

model	r_0	θ	φ	a	b	c	J_0 (cm^{-1})
local spin	19 Å	57.5°	113°	50°	20°	25°	$+1.15 \times 10^{-3}$
point dipole[a]	16.4 Å	71°	127°	60°	10°	25°	$+1.15 \times 10^{-3}$

[a] In this case, r_0 is the distance r_{AB} appearing in Hamiltonian 1.

and the relative orientation of the magnetic axes of the Mo(V) center being specified by the parameters r,θ,φ and the Euler angles a, b, c, respectively. The distances r_{1B} and r_{2B} and the unit vectors $\hat{u}_{1B}$ and $\hat{u}_{2B}$ involved in the local spin Hamiltonian 4 are readily expressed in terms of these parameters and of the iron-to-iron distance, and the exchange interactions are described through the effective parameter J_{AB} defined in eq 8. The experimental spectra were simulated by this procedure, using for the Mo(V) center the g values and line width parameters given by the numerical simulation of the high-temperature spectra and for center 1 the line width parameters $\sigma_x = 0.0072$, $\sigma_y = 0.0046$, $\sigma_z = 0.0046$ deduced from a numerical simulation of the Q-band spectrum of center 1 (not shown). Our previous study of the magnetic interactions between centers A and B in photosystem I has revealed the importance of "*J–r* strain" effects, which can be simply included in the simulation procedure through the relation $J_{AB} = J_{AB}^{\circ} \exp(r - r_0)/r_1$ and a statistical distribution of the intercenter distance r.[9] In the case of xanthine oxidase, the quality of the fit was significantly improved at the three microwave frequencies by using the same relation with $r_1 = 4$ Å and $\sigma_r = 0.22$ Å. The best fits, which were determined by visual inspection, are represented in Figure 8. They were obtained with the set of structural parameters reported in Table 1. At S-band, the numerical simulation was carried out by doubling the line widths of center 1 and by adding to the calculated 1:1 interaction spectrum the signal given by centers 1 belonging to a substantial fraction (55%) of molecules in which the molybdenum atoms are not paramagnetic. It should be pointed out that the position and the relative amplitude of the different lines are very sensitive to the parameters' values and that the simulation of such interacting spectra recorded at three different microwave frequencies introduces very severe restrictions in the parameters' space. The residual differences between calculated and experimental spectra are essentially due to line base distortions and to some approximations made in our simulation procedure, like the neglect of the hyperfine interactions with the molybdenum paramagnetic nuclei and our empirical treatment of the line width.

The local spin model indicates that the center-to-center distance r is equal to 19 Å and that the angle θ between the Fe–Fe and intercenter axes is equal to about 57°. Comparison of the spectra calculated from Hamiltonians 1 and 4 (Figure 4) suggests that, for this geometry, it should be possible to obtain numerical simulations equivalent to those represented in Figure 8 by using the program POINTDIP and an effective distance r_{AB}. A systematic search for the best simulations given by the point dipole model leads to the spectra represented in Figure 10. They were obtained by using a line width treatment identical to that described above and the values of the structural parameters reported in Table 1.

Discussion

In this study, we have considered a system comprising two centers A and B coupled by long-range magnetic interactions. We have shown how the delocalization of the magnetic moments could be accounted for in the Hamiltonian describing these interactions, and we have proposed a local spin model adapted to the case of polynuclear metal centers. This model is based on a detailed description of the pattern of magnetic interactions between all the paramagnetic sites of the system. It was first applied to evaluate the point dipole model that is generally used in the numerical simulation of EPR spectra. The example of dinuclear clusters demonstrates that in some cases the point dipole

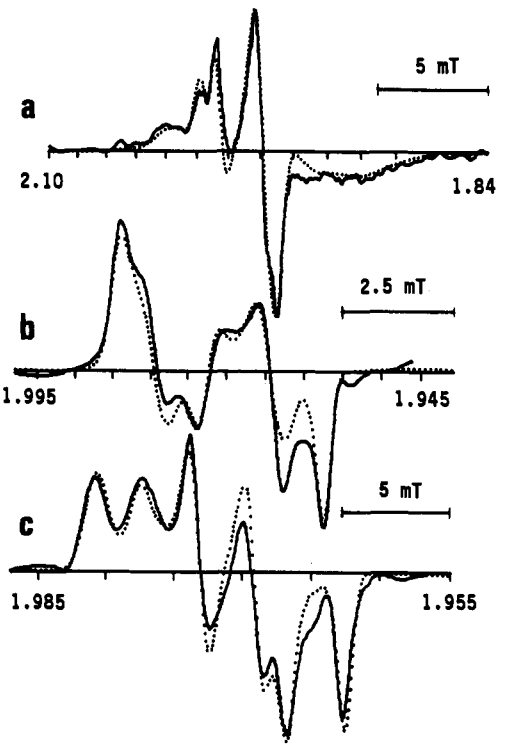

Figure 10. Low-temperature Mo(V) EPR spectra of the desulfo-inhibited form of milk xanthine oxidase with iron–sulfur centers fully reduced. (—) Experimental spectra, same conditions as in Figure 8. (···) Best simulations given by the point dipole model with the structural parameters reported in Table 1 and the following g tensor characteristics: Mo(V) center, same as in Figure 7; center 1, $g_{x,y,z} = 1.894, 1.932, 2.022$.

model can give correct spectral shapes, provided *effective* values are given to the parameters J_{AB} and r_{AB}. These values depend on several contributions and, in general, cannot be directly analyzed in terms of structural information. For some peculiar geometrical configurations, the effective distance r_{AB} becomes infinite. The existence of such "magic distance" configurations could explain some puzzling observations, like the absence of any magnetic interaction between a [2Fe–2S]$^+$ center and a FMN radical separated by a center-to-center distance of about 12 Å in the enzyme phthalate dioxygenase reductase.[29]

The local spin model has been applied to the numerical simulation of EPR spectra resulting from the magnetic interactions between the Mo(V) center and center 1 in the desulfo-inhibited form of the enzyme xanthine oxidase. The realistic character of the model and the very good simulations obtained at three different microwave frequencies with the same set of structural parameters (Figure 8) enable us to propose for the first time a detailed structural arrangement of the two prosthetic groups in the protein (Figure 9 and Table 1). For this arrangement, nearly equivalent simulations can be obtained through the point dipole model (Figure 10). Although the angular parameters given by this model are not very different from those given by the local spin description, the effective distance r_{AB} appears markedly shorter than the center-to-center distance (Table 1). This results from the spin-coupling structure of center 1, an effect that has been emphasized throughout this paper. The value of the effective exchange parameter J_{AB}, which is the same in both models (Table 1), is given by expression 8. In this expression, the superexchange contributions J_{1B} and J_{2B} are expected to be negative (antiferromagnetic), so the positive value of J_{AB} implies that the exchange interactions between the molybdenum center and center 1 are dominated by contributions arising from the ferrous site.

It is interesting to compare the results given by numerical simulations based on the point dipole model to earlier structural

(29) Batie, C. J.; Ballou, D. P.; Correll, C. C. In *Chemistry and Biochemistry of Flavoenzymes*; Müller, F., Ed.; CRC Press: Boca Raton, FL, 1991.

predictions, which were based on the same model and a semiquantitative analysis of the magnetic interactions in xanthine oxidase. In their pioneering work, Lowe and Bray emphasized the weakness of the dipolar contributions and favored a long center-to-center distance of 20–25 Å.[2] This estimation was subsequently revised by Coffman and Buettner[23] and by George.[24] By using crystal-type spectra calculated for some peculiar geometrical configurations and by postulating the existence of a limit function for the distance dependence of the exchange interactions, Coffman and Buettner[23] inferred a much shorter distance, in the range 8–14 Å. A first point concerns the existence of such a limiting function. In the case of polynuclear clusters, we have shown that J_{AB} is an effective parameter which depends on many contributions, so it appears unlikely that its variations can be interpreted through a universal limiting function. Although our value of J_{AB} is similar to that which was deduced from a simple analysis of the spectra,[2,23] the values of the effective distance and of the angular parameters can be determined only by a precise adjustment of the position and the relative amplitude of all spectral features. As a matter of fact, we observe that the numerical simulations based on the point dipole model lead to an effective distance r_{AB} = 16.4 Å (Table 1), which falls between the ranges predicted by the different semiquantitative studies. This clearly illustrates the need for considering the full interaction Hamiltonian without resorting to *a priori* simplifying assumptions and demonstrates that the determination of reliable structural parameters can be obtained only by performing numerical simulations of spectra recorded at different microwave frequencies. Such simulated spectra can now be computed in very reasonable times on even middle-speed machines.

The present study suggests that, when at least one of the interacting species is a polynuclear cluster, the values of the intercenter distance and of the exchange parameter obtained from numerical simulations of EPR spectra based on the point dipole approximation should be interpreted with caution. In contrast, preliminary theoretical investigations indicate that the relative orientation of the magnetic axes and the orientation of the intercenter vector with respect to these magnetic axes are rather well described by the point dipole model, provided the g tensors are weakly anisotropic and the intercenter distance is not too small. Both conditions are expected to be satisfied in most cases for iron–sulfur centers in proteins. A first example is provided by our present study on xanthine oxidase, in which the local spin and point dipole models give very similar angular parameters (Table 1). A second example is provided by our recent analysis of the magnetic interactions between the two [4Fe–4S] centers A and B of photosystems I from the cyanobacterium *Synechocystis* 6803 and from spinach.[9] This analysis, which was based on the point dipole approximation, led to an intercenter distance of about 10 Å and a weak positive (ferromagnetic) exchange coupling. The detailed interpretation of these data should await the application of the local spin model to [4Fe–4S] clusters (see below). However, remarkably enough, the relative orientation of the magnetic axes of centers A and B predicted by the numerical simulation was found to be fully consistent with that determined independently through oriented multilayers experiments. These results were used to define the A–B direction with respect to the membrane normal, which has important implications in the electron-transfer mechanism.[9]

Finally, it will be interesting to test the accuracy of the local spin model by comparing calculated spectra to those given by systems of known geometry. In that case, the model can be used to assign a valence state to the metal ions in polynuclear clusters.

Conclusion

In this paper, we have shown the limit of the point dipole model for describing the magnetic interactions between metal clusters in multicenter proteins, and we have emphasized the advantages of a local spin description. The local spin model was applied to different systems comprising dinuclear centers with trapped valence metal sites. It is interesting to examine to what extent the same model can be applied to systems made of higher nuclearity clusters, like [3Fe–4S] and [4Fe–4S] centers, which are frequently found in biological electron-transfer chains and in metalloenzymes. The extension to $[3Fe–4S]^{+}$ centers in which the three iron atoms are in the ferric state is straightforward, but $[3Fe–4S]^{0}$, $[4Fe–4S]^{+}$, and $[4Fe–4S]^{3+}$ centers contain delocalized valence Fe(III)–Fe(II) pairs, and this raises a new problem for the application of a local spin description. This problem is currently under study by our group.[30] Another general difficulty encountered in the implementation of the local spin model is the need for knowing all local g tensors. These tensors cannot be determined experimentally and must then be extracted from the experimental effective g tensor of the cluster through an appropriate theoretical model. In the preceding section, we have presented an application of this method to the ferric and ferrous sites of a $[2Fe–2S]^{+}$ cluster in xanthine oxidase. The case of higher nuclearity clusters is more involved and will require the help of appropriate theoretical spin coupling models[31,32] as well as experimental information about the orientation of the magnetic axes.[33]

The applications of the local spin model that were discussed above concern polynuclear centers for which the ground state is energetically well separated from excited states and which are weakly coupled by long-range magnetic interactions. It is interesting to note that an attractive local spin model, based on the existence of exchange interactions between a siroheme and one iron site of a [4Fe–4S] cluster, has been proposed by Munck and co-workers[34,35] to explain some peculiar magnetic properties of the enzyme sulfite reductase from *Escherichia coli*. In this model, the intercenter exchange interactions are assumed sufficiently large that, in the fully oxidized state, paramagnetic properties appear at the level of the [4Fe–4S] cluster, whereas the valence state of the iron ions should have led otherwise to a diamagnetic $[4Fe–4S]^{2+}$ center.[34] This range of application of the local spin model is then different from that described in the present study. It should be noted that this model has recently been challenged by Pierik and Hagen,[36] who have proposed a very different interpretation based on the existence of a new iron–sulfur center characterized by an $S = {}^{9}/_{2}$ ground state.

Acknowledgment. We would like to thank Professor R. Cammack for providing facilities for recording low-temperature S-band spectra in his laboratory. Work at The University of Sussex was supported by grants to Professor R. C. Bray from AFRC and SERC.

(30) Bertrand, P. *Inorg. Chem.* **1993**, *32*, 741–745.
(31) Noodleman, L. *Inorg. Chem.* **1991**, *30*, 246–256.
(32) Noodleman, L. *Inorg. Chem.* **1991**, *30*, 256–264.
(33) Gloux, J.; Gloux, P.; Hendricks, H.; Rius, G. *J. Am. Chem. Soc.* **1987**, *109*, 3220–3224.
(34) Münck, E. In *Iron Sulfur Proteins*; Spiro, T. G., Ed.; John Wiley and Sons: New York, 1982; pp 147–175.
(35) Christner, J. A.; Münck, E.; Kent, T. A.; Janick, P. A.; Salerno, J. C.; Siegel, L. M. *J. Am. Chem. Soc.* **1984**, *106*, 6786–6797.
(36) Pierik, A. J.; Hagen, W. R. *Eur. J. Biochem.* **1991**, *195*, 505–516.